Nanocoating Hybrid Polymer Films on Large Quantities of Cohesive Nanoparticles by Molecular Layer Deposition

Xinhua Liang and David M. King
Dept. of Chemical and Biological Engineering, University of Colorado, Boulder, CO 80309

Peng Li
Dept. of Earth and Planetary Sciences, University of New Mexico, Albuquerque, NM 87131

Steven M. George and Alan W. Weimer
Dept. of Chemical and Biological Engineering, University of Colorado, Boulder, CO 80309

DOI 10.1002/aic.11757
Published online February 20, 2009 in Wiley InterScience (www.interscience.wiley.com).

The conformal coating of ultra-thin aluminum alkoxide (alucone) polymer films on primary silica and titania nanoparticles using molecular layer deposition (MLD) in a fluidized bed reactor from 100 to 160 °C is described. In situ mass spectrometry revealed that the growth of alucone MLD films was self-limiting as a function of the individual trimethylaluminum and ethylene glycol exposures. The composition and highly conformal alucone films throughout the surface of both silica and titania nanoparticles were confirmed. The highest growth rate was observed at the lowest sample temperature. Primary nanoparticles were coated individually despite their strong tendency to aggregate during fluidization. Based on the results of chemical and thermogravimetric analysis, the value of x in the formula of $Al(OCH_2CH_2O)_x$ was estimated to be 1.9. The calculated film density slightly increased from 2.0 ± 0.1 to 2.2 ± 0.1 g/cm^3 with the increasing of temperature from 100 to 160 °C. © 2009 American Institute of Chemical Engineers *AIChE J,* 55: 1030–1039, 2009

Keywords: molecular layer deposition (MLD), alucone, nanoparticle, coating, fluidized bed reactor

Introduction

Nanoparticles have gained increased interest in a variety of fields for different applications.[1–3] The performance of several nanoparticle applications could be improved when such particles are coated with ultra-thin inorganic or organic films, which can alter the surface characteristics without degrading the bulk properties of the substrate materials. Many applications are dependent on the molecular properties of the materials. For example, molecule-based semiconductor devices, nonlinear optical devices and sensors are dependent on the molecular properties of the materials, such as the position of molecular energy levels, as well as the macroscopic behavior of the thin film layers;[4–7] nanocoatings of fine capsules can modify the drug release characteristics and provide the physical and chemical protection for the drugs;[7,8] functionalized poly(ethylene glycol) (PEG) layers formed on nanoparticle surfaces can provide for receptor mediated drug

Correspondence concerning this article should be addressed to A. W. Weimer at alan.weimer@colorado.edu.

and gene delivery. This is obtained through PEG-conjugated ligands having a minimal nonspecific interaction with other protein surfactant coatings of polymeric nanoparticles for the controlled delivery of anticancer drugs.[9]

Many techniques, such as the chemical vapor deposition (CVD) method[10] and the Langmuir-Blodgett method[11] have been developed for fabricating polymeric thin films. However, these methods cannot control the order and location of molecular compounds on substrate surfaces, which may inhibit the desired functionality of the coatings. Atomic layer deposition (ALD) methods have been employed to grow films with precise atomic layer control, and many inorganic materials have been grown via ALD including binary compounds.[12–17] The molecular layer deposition (MLD) method,[18,19] which is similar to ALD and is also based on sequential, self-limiting surface reactions, can be utilized to deposit polymer films. In this process, molecules are stacked on substrates one by one in order of preference. The MLD technique offers the same advantages for polymer film deposition as ALD does for ceramic films. In addition, MLD can deposit hybrid polymer films using suitable precursors, such as trimethylaluminum (TMA) and ethylene glycol (EG) for aluminum alkoxide (alucone) hybrid polymer.[20] This vapor-phase method, which operates *in vacuo*, and does not require solvents or catalysts, is a useful and promising technique for the fabrication of functional ultra-thin polymeric layers.

The growth of different polymer MLD films on different substrates has been demonstrated before.[18–28] However, large-scale MLD coating on particles has not been investigated. Many challenges are encountered during MLD on large quantities of nanoparticles. First, the native cohesive properties of the nanoparticles will form agglomerates that are several times larger than the primary particles.[29,30] Therefore, the particles need to be fluidized or agitated to perform the MLD surface reactions in reasonable times, and to prevent the particles from being aggregated by the MLD polymer film. Second, it is difficult to deliver the low-vapor pressure, bulky organic monomer precursor to the reaction chamber and to, subsequently, remove the relatively sticky bifunctional monomers from the primary nanoparticle surfaces. This low-vapor pressure requires the heating of the precursors to obtain sufficient reactant flux. Sufficient reactant flux can be obtained by preheating the organic precursors; however, they tend to decompose at lower temperatures than typical ALD precursors. Third, polymer films fabricated by MLD have more of a tendency to stick than those ceramic films fabricated by ALD, which may increase particle aggregation during the MLD coating process.

The MLD particle coating process can be carried out in a fluidized bed reactor (FBR), which can be used to efficiently deliver gas-phase reactive precursors to bulk quantities of particles. Fluidized bed reactors (FBRs) have been successfully applied for ALD particle coating.[31–37] This type of unit operation is commonly used for various steps throughout powder manufacturing processes. For example, pharmaceutical particles can be manufactured in a fine powder form and dried in an FBR. Integration of the particle MLD process into an existing unit operation would allow for precision polymer coatings on surfaces without significant capital equipment costs. *In situ* mass spectrometry can be used to effectively monitor gaseous product evolution and subsequent unreacted precursor breakthrough.[37] This makes the combined system unique as it enables *in situ* growth of a number of controllable and uncontaminated polymer films without risk of cross-contamination between the two systems.

Alucone is a typical inorganic/organic hybrid polymer, which has been fabricated by sol-gel (solution-gelation) reaction of alkylaluminum molecules with an organic alcohol, and can also be used to produce γ-Al_2O_3 by thermolysis.[38] Dameron et al.[20] first investigated the chemistry of alucone MLD using TMA and EG, and demonstrated alucone MLD on ZrO_2 particles (~30 nm), and $BaTiO_3$ particles (~200 nm) at a small (<0.1 g) scale in a viscous flow reactor. In this study, large-scale alucone MLD coating on fine particles using the reaction of TMA with EG in a scalable FBR was demonstrated.

Experimental Details

Alucone MLD on nanoparticles

The MLD process was carried out in a vibrating FBR, as shown in Figure 1. The reactants are TMA and EG. The proposed MLD half-reactions between TMA and EG are listed as follows[20]

$$\mathrm{A}: -\mathrm{OH}^* + \mathrm{Al(CH_3)_3} \rightarrow -\mathrm{OAl(CH_3)_2}^* + \mathrm{CH_4} \quad (1)$$

$$\mathrm{B}: -\mathrm{AlCH_3}^* + \mathrm{OHCH_2CH_2OH} \rightarrow -\mathrm{AlOCH_2CH_2OH}^* + \mathrm{CH_4} \quad (2)$$

Here the asterisks designate the surface species. The fluidized bed was 3.5 cm in diameter. There was a 10 μm pore-size porous metal disc in the middle of the reactor as the gas distributor. The reactor was encased by a clamshell-type furnace and bolted to a platform that rested on four large springs. The reactor was maintained at low pressure by a

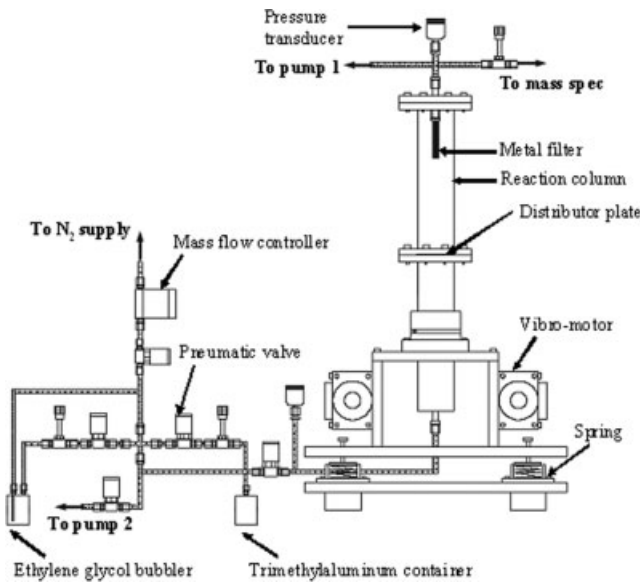

Figure 1. Schematic diagram of the molecular layer deposition-fluidized bed reactor.

vacuum pump, and the dosing header could also be pumped down directly using a smaller separate pump. A vibration system was utilized to overcome some of the interparticle forces and improve the quality of fluidization. High-purity N_2 gas was used as the purge gas to remove the unreacted precursor and any byproducts formed during the reaction. Its flow rate was controlled by a mass-flow controller. Baratron® capacitance manometers (MKS Instruments) were located below the distributor plate and at the outlet of the reactor column to measure the pressure drop across the bed of particles. All valves used to provide the transient dosing were automatically controlled through LabView® (National Instruments). Pressure measurements were recorded to monitor the progress of each dosing cycle.

MLD of ultra-thin alucone films was carried out on 250 nm spherical silica particles (Sigma Aldrich) and 160 nm anatase titania particles (Millennium Chemicals). For a typical run, 10 g of particles were loaded into the reactor. The reaction temperature ranged from 100 to 160°C. The feeding lines were kept at ~80°C to avoid excessive adsorption of EG on the internal walls of the system that could promote CVD side-reactions. The minimum pressure inside the reactor was ~10 Pa, and the minimum fluidization superficial gas velocity was determined by measuring the pressure drop across the bed vs. the N_2 superficial gas velocity. One example of titania particle fluidization at 100°C is shown in Figure 2. During the MLD reaction, TMA (97%, Sigma Aldrich) was fed through the distributor of the reactor, based on the driving force of its room-temperature vapor pressure. The flow rate of TMA was limited using a needle valve, while ensuring that the TMA pressure at the base of the reactor was high enough to promote particle fluidization.

The room-temperature vapor pressure of EG (anhydrous, 99.8%, Sigma Aldrich) is very low, and is much lower than that required for the fluidization of reasonable bed masses. Heating the EG liquid raises its vapor pressure in accordance with the Antoine equation. The required operating pressures were achieved using this strategy, however, the flow rate control offered by the needle valve was then insufficient to prevent the pure-component EG vapor stream from flooding into the system. Since EG is a sticky molecule, it can be very difficult to remove any overdosed vapor from the particle surfaces or the reactor walls. A bubbler was employed to dilute the heated EG vapor stream, and allowed for vapor delivery to the reactor in a controllable fashion, and prevented the overdose of the precursor. The bubbler inlet was controlled using a mass-flow controller (MKS Instruments) to allow a calibrated amount of N_2 to be bubbled through the precursor reservoir. In this case, a flow rate of 4 sccm of N_2 was sufficient to deliver EG, which was preheated to 80°C, to the reactor. The utilization of a bubbler is very important for MLD process operation, as it can easily maintain and control stable supply rates of preheated gaseous molecular precursors. This procedure may also be required for dosing precursors into industrial scale FBRs, which would operate at much higher flow rates to achieve pressure drops associated with large-bed masses.

For good operational growth control, an internal quadrupole mass spectrometer (Stanford Research Systems) was connected to the outlet side of the reactor, as shown in Figure 1. The m/z peaks of interest (i.e., primary and fragmentation peaks) for the precursors were 42, 57, 72 for TMA, 31, 33, 62 for EG, and 16 for CH_4. This real-time monitoring strategy can effectively monitor gaseous product evolution and subsequent unreacted precursor breakthrough, and allow for optimizing the dose time of precursors to prevent process overruns and excess precursor waste. The process is commercially significant since it can operate in a simple process for practical large scale applications.

Before the reaction, the particles were dried at 120°C under continuous N_2 flow for 3 h. A typical coating cycle consisted of the following sequence: TMA dose, N_2 purge, evacuation; EG dose, N_2 purge, evacuation. In this manner, there was no overlap between the two reactants, such that no undesirable CVD side-reactions could occur.

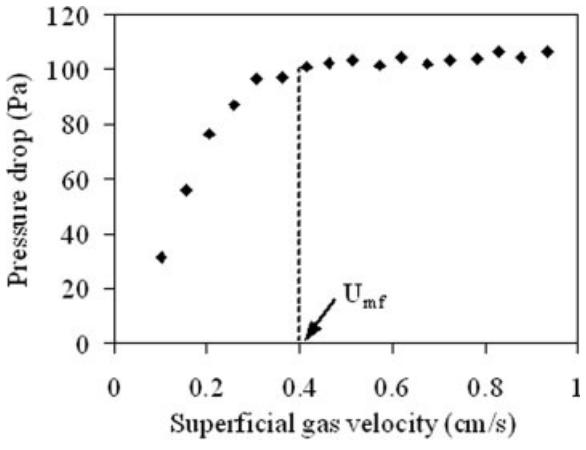

Figure 2. Pressure drop across the fluidized bed vs. superficial gas velocity for titania nanoparticles at 100°C and reduced pressure.

Analysis

The composition of MLD films was analyzed by energy dispersive spectroscopy (EDS) using a JEOL JSM-7401F field emission scanning electron microscope (FESEM) coupled with an EDAXS detector unit for elemental analysis. The coated particles were visualized with a JEOL 2010F 200 kV Schottky field emission transmission electron microscope equipped with an Oxford detector unit for elemental analysis while imaging. Inductively coupled plasma atomic emission spectroscopy (ICP-AES) was performed using an Applied Research Laboratories ICP-AES 3410+. ICP-AES is a convenient technique that can be used to measure the mass content of metals (in parts per million) in a sample dissolved in a strong acidic or basic solution. Here the metal of interest was Al, and a strong base solution (NaOH) was used to dissolve the alucone film from the substrate particles. The substrate particle (TiO_2 or SiO_2) itself will not dissolve at normal laboratory conditions. The specific surface area of the particles was obtained using a Quantachrome Autosorb-1. A Theta Gravitronic II thermogravimetric analyzer (TGA) was used to measure the mass change of the coated nanoparticles during oxidation. The powder sample was loaded into an alumina crucible, suspended from a microbalance by a Pt wire,

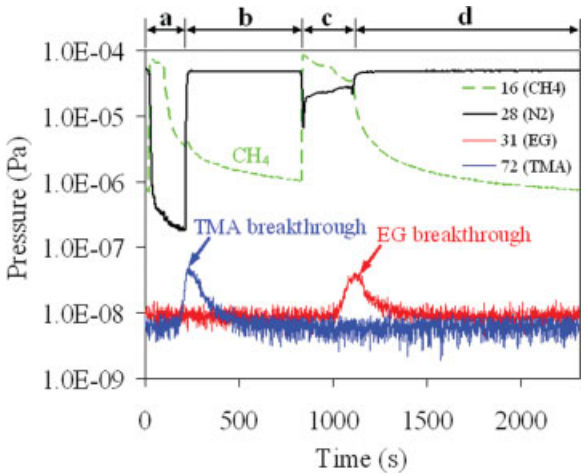

Figure 3. *In situ* mass spectrometry results during one complete MLD cycle: (a) TMA dose, (b) N_2 purge, (c) EG dose, and (d) N_2 purge.

There was 10 s of evacuation between N_2 purge and precursor dose. [Color figure can be viewed in the online issue, which is available at www.interscience.wiley.com.]

and heated in a tube furnace from 25 to 1,000°C at the rate of 10°C min^{-1}. An 85:15 ratio N_2:O_2 stream was allowed to flow downward across the crucible at 200 sccm to promote the oxidation of the hybrid polymer films.

Results and Discussion

Self-limiting surface reactions

The *in situ* mass spectrometry results of alucone MLD on silica particles at 100°C, shown in Figure 3, indicate that the chemistry of TMA and EG MLD was self-limiting, which is similar to ALD chemistry.[12–16] When TMA was dosed into the reactor, there was an instantaneous increase of the CH_4 byproduct. Since the pressure of the reaction product remained relatively constant, the methane generation rate was stable. It is clear that all TMA entering the reactor was completely utilized until the time at which the TMA signal increased, which is called the "breakthrough" time. Beyond this time, the probability of reactive precursor molecules locating unreacted surface sites decreased. The extent of surface reaction at the point of breakthrough is dominated by the reactivity of the precursor. TMA is an extremely reactive precursor and as such, very high surface conversions, in some instances greater than 98%, have been observed at the point of breakthrough.[37] Evidence that supports complete surface conversion is that CH_4 signal decreased significantly with the increasing of TMA signal, and the negligible change in methane evolution rate after the TMA dose was stopped. Just after the TMA breakthrough time, the TMA dose was stopped, and N_2 was fed into the reactor at a flow rate of 5 sccm to purge any residual reaction product or unreacted TMA from the system. After the 600 s N_2 purge, EG was dosed and the CH_4 signal increased again. As the EG dose proceeded, the reaction product began to decrease, and the signal of EG (m/z = 31) appeared. Since CH_4 signal did not drop significantly with the increasing of EG signal, full surface conversion may be not obtained. This underdosing was intentional, in order to minimize the amount of unreacted EG that flowed through the system due to the sticky nature of the precursor and the removal difficulties explained previously. During both precursor doses, it is apparent that the reactions were self-limiting and self-terminating, because the reaction products increased and then decreased while the reactants were still being dosed. If these reactions had not been self-limiting, the products would continue to be generated as long as the reactants were dosed.

Test for composition and conformality of alucone films

Alucone MLD films have been coated on silica and titania nanoparticles. In order to determine the composition of MLD films, the uncoated and coated silica particles were analyzed by EDS. The results are shown in Figure 4. For the uncoated silica particles, only O and Si signals were present, as shown in Figure 4a, and the trace presence of carbon was from the

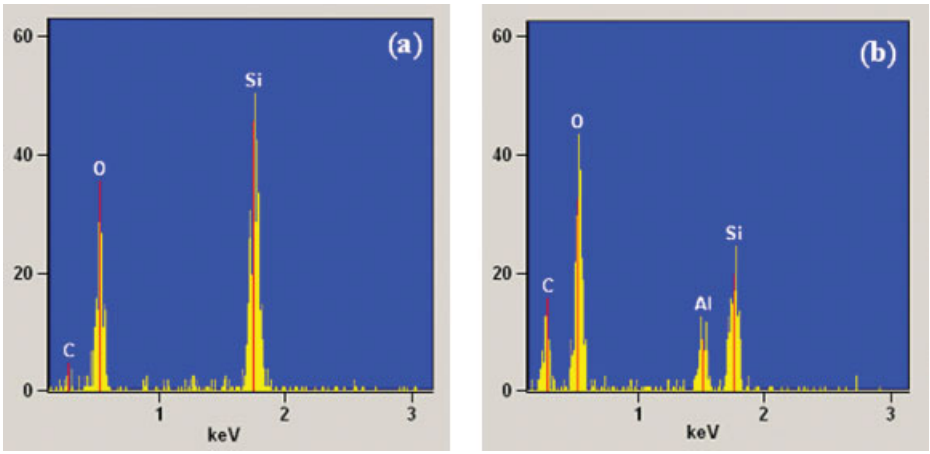

Figure 4. EDS spectra of (a) uncoated, and (b) 50 cycles MLD coated silica nanoparticles.

[Color figure can be viewed in the online issue, which is available at www.interscience.wiley.com.]

background. In contrast, for the 50 cycles MLD coated silica particles (Figure 4b), there was a strong peak of Al, and the presence of both carbon and oxygen was much more pronounced. This is a direct confirmation of the presence of alucone MLD films, which have a backbone structure of the —Al—O—CH_2—CH_2—O— species.

Scanning transmission electron microscopy (STEM) images of the silica particles coated with 50 MLD cycles at a reaction temperature of 100°C showed the presence of extremely conformal alucone films, as displayed in Figure 5. The measured thickness of the film was 25 ± 0.5 nm, which represents a growth rate of ~0.50 nm/cycle at 100°C. The composition of the MLD films was determined by EDS elemental nanoanalysis, as shown in Figures 5c and d. Similarly, TEM images (Figures 6a and b) of the titania particles coated with 20 MLD cycles at 160°C also exhibited extremely conformal alucone film growth. The thickness of the film grown at 160°C was 7 ± 0.3 nm, which represents a slightly lower growth rate of ~0.35 nm/cycle at that temperature. The composition of MLD films was also determined by elemental nanoanalysis, as shown in Figures 6c and d. The thickness of alucone films on TiO_2 particles after 20 cycles at 100°C was 10 ± 0.4 nm observed by TEM, which represents a growth of ~0.50 nm/cycle at 100°C.

Theoretically, the growth rate per cycle is based on the nucleation site density. For these self-limiting reactions, the theoretical maximum coverage is one monolayer. Submonolayer coverage would happen when the surface reaction may be somewhat incomplete leaving the chemisorption layer short from saturation, which could be caused by relative low reaction speed, or incomplete surface saturation due to the steric hindrance of bulky reactant molecules. In another case, slight thermal decomposition of precursors or localized CVD would result in higher film growth rate. In this case, it is hypothesized that the variation in growth rate was predominantly due to temperature, rather than the substrate particle size or substrate material. These growth rates were much higher than the growth rate of 0.13 nm/cycle obtained by alucone MLD on $BaTiO_3$ particles (~200 nm) at 135°C, at a small (<0.1 g) scale in a viscous flow reactor.[20] The reason for the difference will be discussed later.

Linear growth of MLD films

The aluminum concentrations on the titania and silica particles were analyzed by ICP-AES, as shown in Figures 7a and b, respectively. Figure 7a shows that the concentration of aluminum on the titania particle surface is almost directly

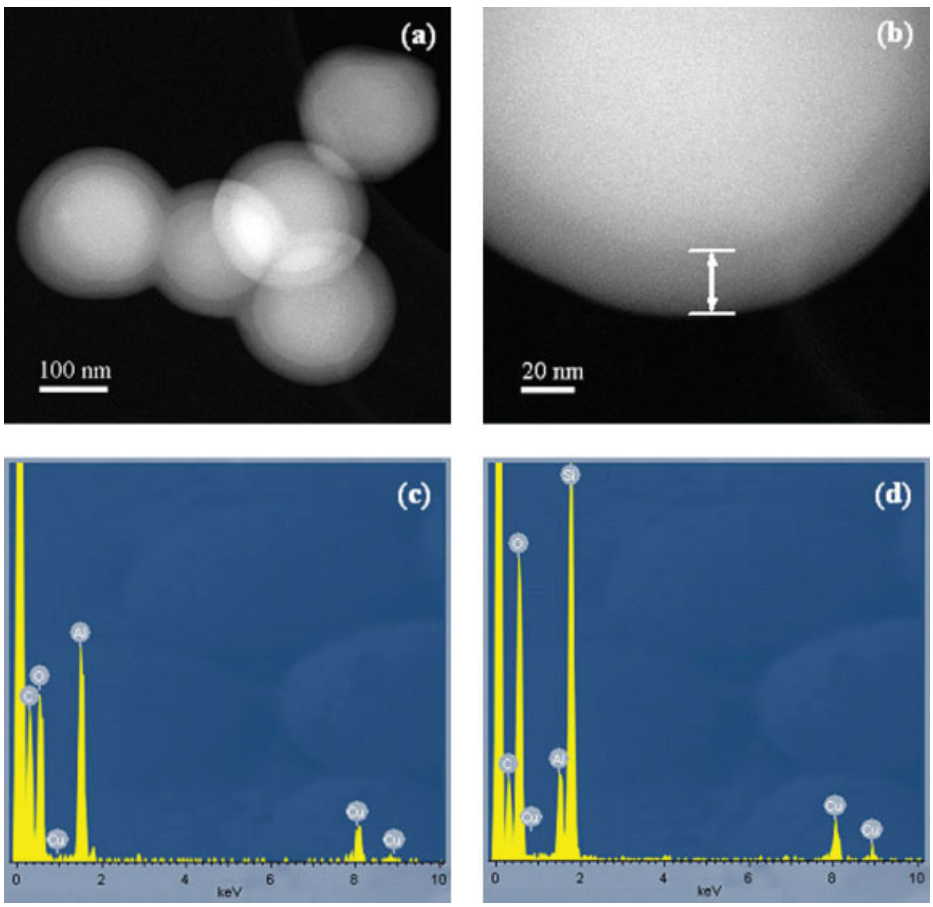

Figure 5. (a and b) STEM images of 50 cycles MLD coated silica nanoparticles at 100°C, and EDS spectra of (c) the particle surface, and (d) the particle substrate.

[Color figure can be viewed in the online issue, which is available at www.interscience.wiley.com.].

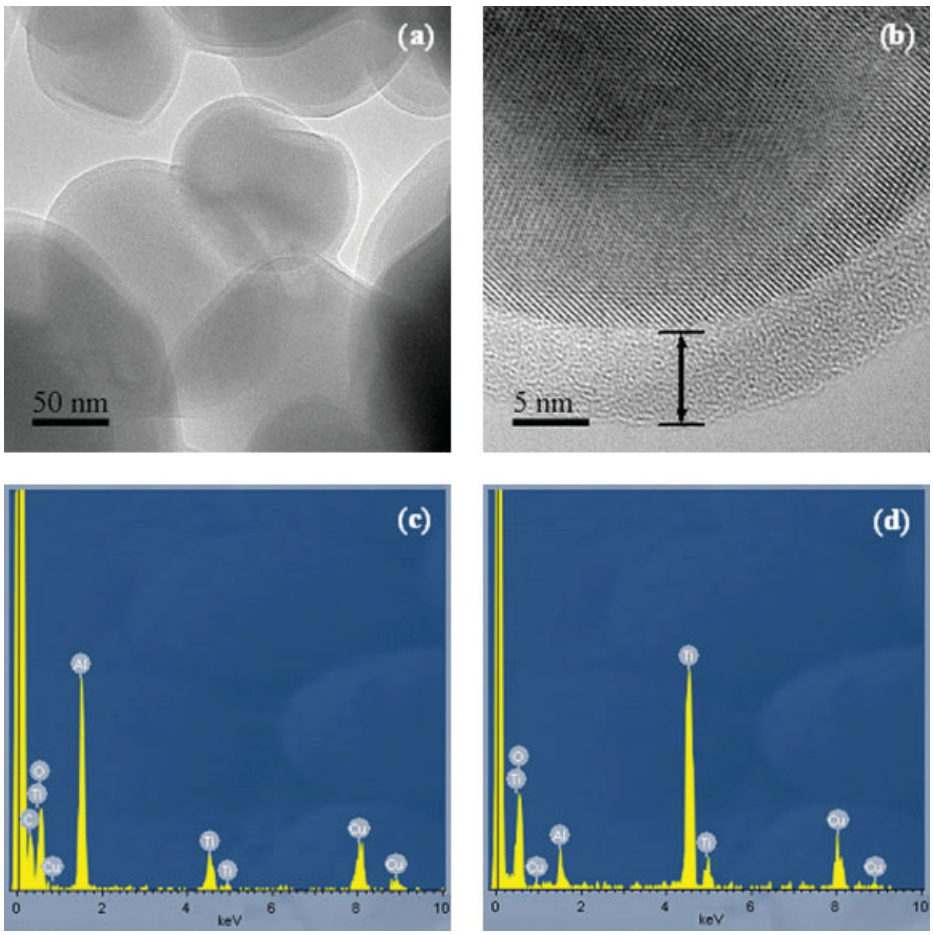

Figure 6. (a and b) TEM images of 20 cycles MLD coated titania nanoparticles at 160°C, and EDS spectra of (c) the particle surface, and (d) the particle substrate.

[Color figure can be viewed in the online issue, which is available at www.interscience.wiley.com.].

proportional to the number of coating cycles. Since the coating thickness is very small compared to the nanoparticle radius, it indicates a constant growth rate of alucone hybrid films and a linear dependence between the film thickness and the number of growth cycles. In other words, the film thickness and the molecular weight of the polymer can be controlled by the number of reaction cycles. Similar results are observed for MLD coated silica particles, as shown in Figure 7b. Therefore, no nucleation period was needed for alucone MLD growth on silica and titania particles, and deposition began during the first cycle. This is because native hydroxyl groups are present on silica and titania particle surfaces, and can react with TMA to initiate the MLD film growth during the first coating cycle. It is clearly indicated from these results that the increase in the thickness of the film is due to a chain-extending process from the substrate surface and molecule-by-molecule growth of conjugated hybrid polymer films can be achieved on substrates by MLD.

Temperature dependence of film growth

Separate runs of 20 cycles of MLD coating at the temperatures of 100, 120, 140, 160 °C were performed on equivalent substrate batch sizes. The TMA and EG reactant exposures were nearly identical for all of these sample temperatures. The resulting aluminum concentrations of the MLD coated titania particles at different temperatures are listed in Figure 8. With increasing reaction temperature, the Al concentration of the samples decreased, which means alucone film growth rates were higher at lower temperatures, and varied in approximate linear-fashion, but this temperature dependence of alucone MLD growth rate was relatively weak. This result corroborates the inverse temperature dependence on alucone growth rate observed from TEM imaging. This temperature-dependent film growth rate suggests that the residence time of the reactants on the surface is important in determining the film growth rate.[27] The reaction rate decreases with decreasing residence time of the precursor on particle surfaces at higher temperatures. This behavior can be explained by precursor-mediated adsorption effects, which are generally used to explain reactions that decrease with increasing temperature.[27,39] Precursor-mediated adsorption kinetics have been observed previously for the initial sticking coefficients of adsorbates on semiconductor surfaces.[40,41]

Dameron et al.[20] reported that the growth rate varied from 0.4 nm/cycle at 85°C to 0.04 nm/cycle at 175°C, which is much more severe than the temperature dependence of alucone MLD growth rate obtained in this study. The difference

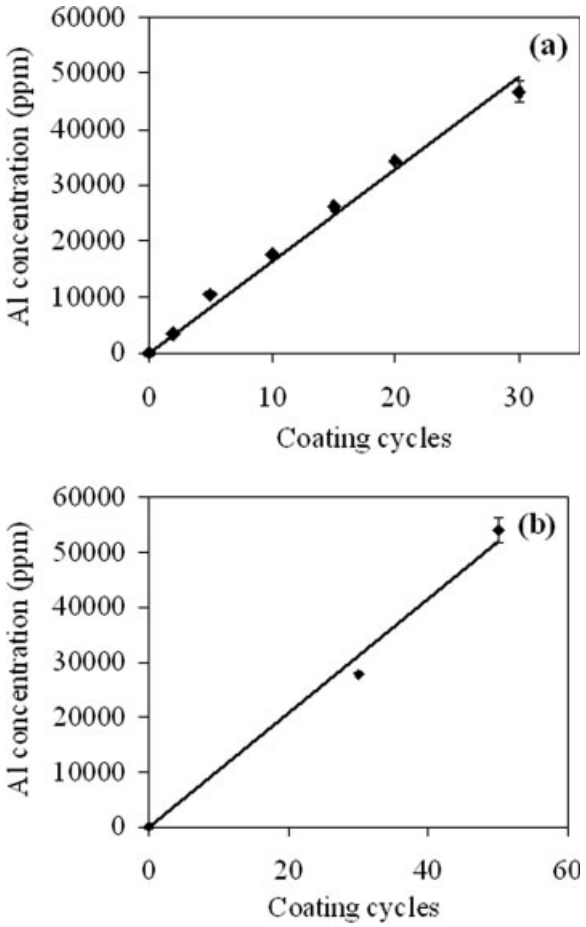

Figure 7. Aluminum concentration on (a) titania, and (b) silica particles vs. coating cycles.

of temperature dependence and alucone MLD film growth rate can be explained by the different reaction environment. The residence time of both precursors on the substrate surface is dependent on the reaction temperatures, and the ability to vacuum the system down, since EG is sticky and TMA can adsorb into the polymer films. For the small-scale alucone MLD process demonstrated by Dameron and coworkers, one layer of $BaTiO_3$ particles was pressed into a tungsten grid, which was similar to a flat substrate. It would be relatively easy to pull the unreacted precursors off the substrate surface and vacuum the system down. Therefore, the residence time of precursors was mainly dependent on reaction temperature, and the film growth rate was much lower at higher temperatures. For this large-scale MLD process here, there was a bed of particles, during the precursor dosing or vacuum purging process, the precursor species left one particle surface were possible to stick on another particle surface, therefore, in a whole, the residence time of precursors would not change a lot with the change of temperatures. Although the residence time of precursors is dependent on reaction temperature, it is losing its significance to determine the film growth rate at different temperatures in this case. The unreacted TMA or EG molecules adsorbing or sticking on the particle surface could react with the incoming precursor molecules, and localized CVD reaction could happen, which can contribute to the higher film growth rate.

Conformal coating of primary nanoparticles

Strong interparticle forces exist between cohesive nanoparticles, and aggregate formation tends to complicate the control of nanopowder-based manufacturing processes. The biggest challenge in trying to individually coat primary nanoparticles is to overcome their natural tendency to form soft agglomerates, primarily due to van der Waals attractive forces. It has been recently shown that nanoparticles fluidize as micron-sized agglomerates.[29,30] In MLD coating processes, liquid bridging, one of the strongest interparticle forces, also becomes problematic due to low operating temperature requirements and the use of sticky precursors. BET surface area analysis was performed to ensure the coating did not permanently bind the individual particles into aggregates. For the uncoated titania particles, the surface area was 9.47 ± 0.24 m^2/g, and decreased to 8.51 ± 0.31 m^2/g after 20 MLD cycles deposited at 100 °C. Theoretically, because of the different density of the coatings and the substrate, the surface area of the titania nanoparticles after 20 coating cycles should slightly increase. In this case, a slight decrease in surface area was observed, indicating a small degree of permanent aggregation, which could be caused by small degree of localized CVD. Only a drastic decrease in specific surface area would signify a high degree of aggregation, which indicates that the majority of titania particles functionalized by the alucone MLD films were coated on primary particles.

Although one of the MLD precursors is very sticky, and the nanoparticles are highly cohesive, the individual particles were predominantly coated, as opposed to necking multiple particles together in the fluidized bed. This phenomenon can be explained by a behavior called dynamic aggregation, which is observed during fluidization of nanoparticles when interparticle forces can be successfully overcome.[30,32] Dynamic agglomerates partially break apart and reform due to constant solids recirculation and gas flow through the bed of particles. The utilization of a bubbler dilutes the sticky EG

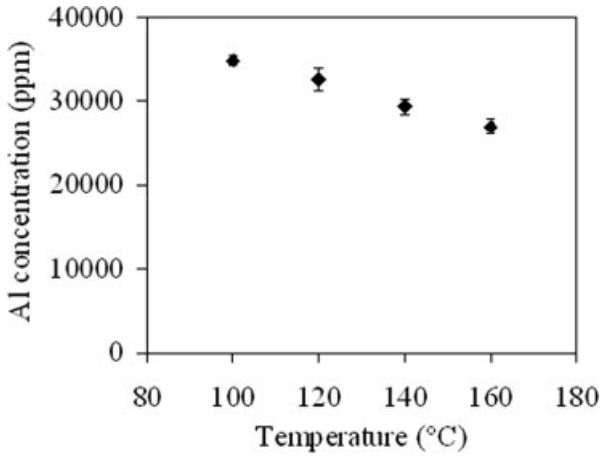

Figure 8. Aluminum concentration on the MLD coated titania particles at different reaction temperatures.

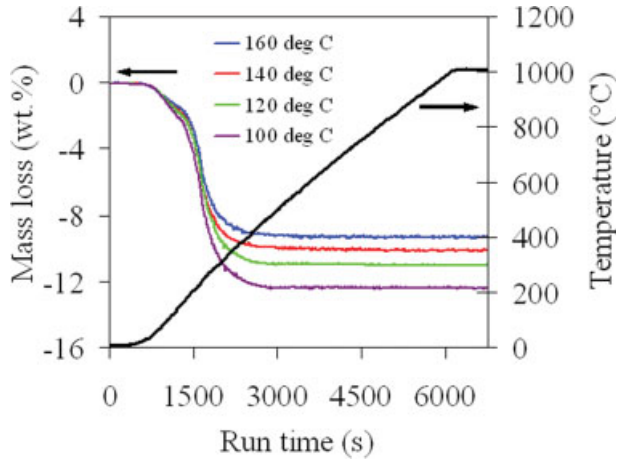

Figure 9. Thermal gravimetric analysis of titania particles with 20 MLD coating cycles at different temperatures.

[Color figure can be viewed in the online issue, which is available at www.interscience.wiley.com.]

vapor, which can help mitigate liquid bridging effects and can improve the solids recirculation. Mechanical vibration improves the fluidization quality by generating a pressure fluctuation that is transferred to the bed via a gas gap.[42] This externally supplied energy helps to partially overcome interparticle forces, and serves to reduce the average size and increase the disengagement rate of particles within agglomerates in the bed, which ultimately increases the frequency of particle impacts. Even though this breakage is partial and temporary during a single collision event, due to recirculation and frequent impacts, the entire surface area of each of the primary particles will be eventually exposed and the individual nanoparticles can be coated.[32]

Thermolysis of alucone films

The thermal decomposition of the alucone hybrid films was studied by TGA in air. As shown in Figure 9, the alucone films began to decompose at 80°C with no further mass loss observed above 450°C. The decomposition appeared to occur in two steps. The first step occurred over a temperature range of 80–200°C, which was caused by dehydration and loss of ethoxy groups on the particle surface. The second step happened over a temperature range of 200–400°C, which was caused by polymer decomposition in the MLD films. The final mass after pyrolysis in air at 1,000°C is lower than the results calculated from the Al concentration analysis if the MLD films have a stoichiometric formula of $Al(OCH_2CH_2O)_{1.5}$. Therefore, the fabricated hybrid film does not have a stoichiometric structure, and the value of x in the formula $Al(OCH_2CH_2O)_x$ of MLD films will be higher than the stoichiometric value of 1.5.

Structure and density of alucone films

The value of x in the formula $Al(OCH_2CH_2O)_x$ of MLD films can be estimated using the measured mass loss of particles during the TGA test and Al concentration on particles based on ICP-AES measurement. During the TGA oxidation process, all carbon and hydrogen in polymer will be burned out and Al will be converted to alumina. Since the MLD film itself contains enough oxygen atoms, it is safe to assume that no additional oxygen molecules are needed to convert Al to alumina. Therefore, the total mass of MLD films is equal to the mass loss during the TGA test (the substrate mass remains unchanged) plus the mass of alumina left on the particle surface, which can be calculated based on ICP-AES Al concentration on particles. Consequently, the value of x in the formula $Al(OCH_2CH_2O)_x$ of MLD films can be estimated by the following equations

$$\frac{[\text{Mass of MLD film}]_g}{(27+60x)_{g/mol}} = \frac{[\text{Mass of Al}]_g}{27_{g/mol}} \quad (3)$$

$$\frac{1}{(27+60x)_{g/mol}} = \frac{[\text{Mass of Al}]_g}{[\text{Mass of MLD film}]_g \times 27_{g/mol}} = a \quad (4)$$

$$x = \frac{(1/a - 27)}{60} \quad (5)$$

Dameron et al. found that the alucone film was not stable, and the structure of the film may change in the presence of water,[20] but there should be no aluminum loss of the MLD film, so the instable property of alucone film would not affect the ICP-AES results. Also, in order to prevent the structure change or mass loss of the film, the samples were stored *in vacuo* before TGA tests. Figure 10 shows the value of x in the formula $Al(OCH_2CH_2O)_x$ of MLD films fabricated at different temperatures. It shows that there was not a significant shift in the value of x over the deposition temperature range used here, and the average value of x is 1.9. The constant x value indicates that alucone MLD films fabricated at different temperatures have a similar molecular structure. Given the low-vapor pressure and sticky property of EG monomer and relatively low reaction temperatures, EG molecules may condense on the surface to form a multimolecular layer accumulate on the particle surface, which can be an explanation of higher x values than the stoichiometric value of 1.5. To the best of our knowledge, ICP-AES is a very accurate method to test the aluminum concentration. However,

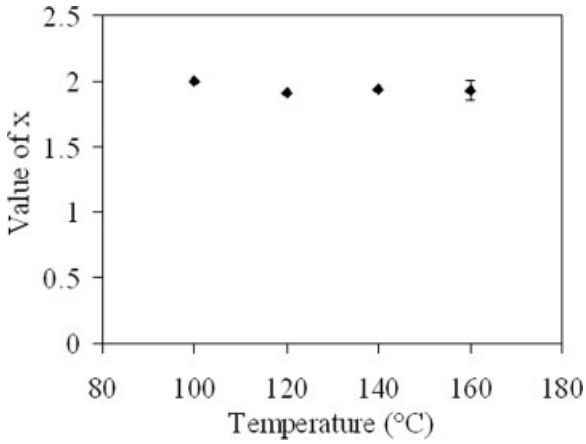

Figure 10. The value of x in the formula $Al(OCH_2CH_2O)_x$ of MLD films fabricated at different temperatures.

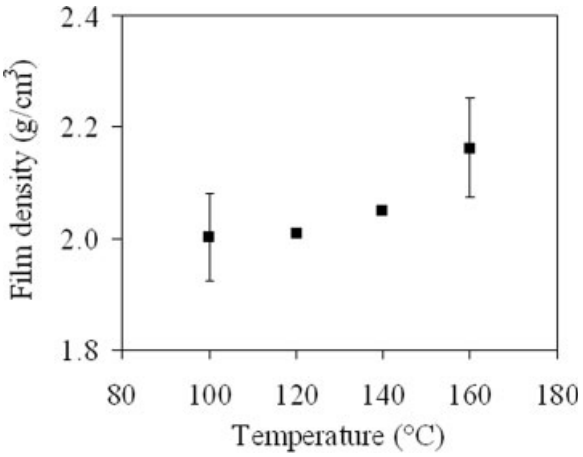

Figure 11. The calculated density of MLD films fabricated at different temperatures.

lower value of aluminum ICP-AES concentration than actual value could also lead to a higher x value. The constant x value across a wide temperature range can be explained by the similar residence time of precursors on substrate surfaces, as discussed previously.

It is difficult to directly measure the density of MLD films on particles. The density of MLD films can be estimated on the basis of the polymer film mass and the film volume, which can be calculated based on the particle surface area and film thicknesses observed by TEM. Here the surface area (9.47 m^2/g) of uncoated particles was used. As shown in Figure 11, there was not a significant shift in the value of the calculated density over the deposition temperature range used here. With the increase of reaction temperature from 100 to 160 °C, the film density slightly increased from 2.0 ± 0.1 to 2.2 ± 0.1 g/cm^3, which also indicates the similar molecular structure of alucone MLD films fabricated at different temperatures. These calculated densities were higher than the density of 1.5 g/cm^3 of alucone MLD films grown on flat silicon substrates measured by X-ray reflectivity (XRR).[20] The inaccuracy of estimated film volume could be attributed to this difference, since small degree of particle aggregation happened. This difference could also be caused by the high ratio of curvature of fine particles, and less steric effect occurred during the adsorption step of the reaction, thus potentially denser films may be produced.

Conclusions

Large quantities of cohesive silica and titania nanoparticles were conformally coated with aluminum alkoxide (alucone) ultra-thin films using molecular layer deposition (MLD) in a vibrating fluidized bed reactor. The deposition chemistry and properties of alucone MLD films were investigated. *In situ* mass spectrometry studies showed that the alucone MLD film growth was the result of self-limiting surface reactions. The composition of alucone hybrid nanolayers was confirmed by EDS. Highly conformal and uniform films on titania and silica particles were observed via TEM and z-contrast STEM, respectively. The thickness and molecular weight of polymeric thin films can be effectively controlled by the number of reaction cycles during the sequential vapor deposition process. The growth rate varied from 0.5 nm/cycle at 100 °C to 0.35 nm/cycle at 160 °C, which is much higher than the growth rate of MLD films grown on particles at a small scale. The higher film growth rate could be caused by localized CVD, since EG is sticky and TMA can adsorb into the polymer films. The growth rates decreased at higher substrate temperatures. The surface area of nanoparticles was not significantly affected by the coating process. Primary nanoparticles were coated individually due to their dynamic aggregation behavior.

A combination of the gravimetric methods and chemical analysis of the MLD films makes it possible to determine the stoichiometry of surface nanostructures produced by MLD. The stoichiometric composition of the hybrid films has been calculated with respect to the aluminum concentration in the MLD film and total mass loss of the MLD film during the TGA oxidation test. The value of x in the formula $Al(OCH_2CH_2O)_x$ of fabricated MLD films is 1.9 at the temperature range of 100–160°C. The calculated film density slightly increased from 2.0 ± 0.1 to 2.2 ± 0.1 g/cm^3 with the increase of temperature from 100 to 160 °C.

This work presents herein, the first attempt at placing ultra-thin conformal polymer films on nanoparticles at large-scale. MLD has the advantage of low deposition temperature, precision thickness control and excellent conformality. The applications that can utilize conformal polymer films with monomer level thickness control are expected to grow. This approach can be applied, in principle, to other copolymer films or inorganic/organic hybrid films on different substrates, and it will open the door to the design of new 3-D (three-dimensional) molecular architectures on surfaces, which has the potential to add novel functionalities to a variety of industrial and pharmaceutical applications, such as molecular electronics, electrocatalysts, and pharmaceutical coating applications.

Acknowledgments

This work was partly supported by the National Science Foundation under Grant 0400292, the Department of Energy under STTR Grant DE-FG02-03ER86157 and the Department of Education Graduate Assistance in Areas of National Need program. Any opinions, findings, and conclusions or recommendations expressed in this work are those of the authors and do not necessarily reflect the views of these government organizations. The authors thank Fredrick G. Luiszer at the University of Colorado for providing the ICP-AES analysis.

Literature Cited

1. Bruchez M, Moronne M, Gin P, Weiss S, Alivisatos AP. Semiconductor nanocrystals as fluorescent biological labels. *Science*. 1998;281:2013–2016.
2. Panyam J, Labhasetwar V. Biodegradable nanoparticles for drug and gene delivery to cells and tissue. *Adv Drug Delivery Rev*. 2003;55:329–347.
3. Daniel MC, Astruc D. Gold nanoparticles: Assembly, supramolecular chemistry, quantum-size-related properties, and applications toward biology, catalysis, and nanotechnology. *Chem Rev*. 2004;104:293–346.
4. Bohler A, Urbach P, Ammermann D, Kowalsky W. Organic molecular beam deposition: technology and applications in electronics and photonics. *Mater Sci Eng B-Solid State Mater Adv Technol*. 1998;51:58–65.
5. Andreasson M, Ilver L, Kanski J, Andersson TG. Organic molecular beam deposition system and initial studies of organic layer growth. *Physica Scripta* 2006;T126:1–5.

6. Abe M, Michi T, Sato A, Kondo T, Zhou W, Ye S, Uosaki K, Sasaki Y. Electrochemically controlled layer-by-layer deposition of metal-cluster molecular multilayers on gold. *Angewandte Chemie-Int Edition*. 2003;42:2912–2915.
7. Theobald JA, Oxtoby NS, Phillips MA, Champness NR, Beton PH. Controlling molecular deposition and layer structure with supramolecular surface assemblies. *Nature*. 2003;424:1029–1031.
8. Bose S, Bogner RH. Solventless pharmaceutical coating processes: A review. *Pharma Develop Technol*. 2007;12:115–131.
9. Otsuka H, Nagasaki Y, Kataoka K. PEGylated nanoparticles for biological and pharmaceutical applications. *Adv Drug Delivery Rev*. 2003;55:403–419.
10. Kubono A, Okui N, Tanaka K, Umemoto S, Sakai T. Highly oriented polyamide thin-films prepared by vapor-deposition polymerization. *Thin Solid Films*. 1991;199:385–393.
11. Sanchez-Gonzalez S, Ruiz-Garcia J, Galvez-Ruiz MJ. Langmuir-Blodgett films of biopolymers: a method to obtain protein multilayers. *J Colloid Interface Sci*. 2003;267:286–293.
12. Suntola T, Hyvarinen J. Atomic layer epitaxy. *Annual Rev Mater Sci*. 1985;15:177–195.
13. George SM, Ott AW, Klaus JW. Surface chemistry for atomic layer growth. *J Phys Chem*. 1996;100:13121–13131.
14. Ferguson JD, Weimer AW, George SM. Atomic layer deposition of boron nitride using sequential exposures of BCl_3 and NH_3. *Thin Solid Films*. 2002;413:16–25.
15. Ferguson JD, Weimer AW, George SM. Atomic layer deposition of SiO_2 films on BN particles using sequential surface reactions. *Chem Mater*. 2000;12:3472–3480.
16. Ferguson JD, Yoder AR, Weimer AW, George SM. TiO_2 atomic layer deposition on ZrO_2 particles using alternating exposures of $TiCl_4$ and H_2O. *Appl Surf Sci*. 2004;226:393–404.
17. Liang XH, Zhan GD, King DM, McCormick JA, Zhang J, George SM, Weimer AW. Alumina atomic layer deposition nanocoatings on primary diamond particles using a fluidized bed reactor. *Diamond Relat Mater*. 2008;17:185–189.
18. Yoshimura T, Tatsuura S, Sotoyama W. Polymer-films formed with monolayer growth steps by molecular layer deposition. *Appl Phys Lett*. 1991;59:482–484.
19. Yoshimura T, Tatsuura S, Sotoyama W, Matsuura A, Hayano T. Quantum wire and dot formation by chemical vapor-deposition and molecular layer deposition of one-dimensional conjugated polymer. *Appl Phys Lett*. 1992;60:268–270.
20. Dameron AA, Seghete D, Burton BB, Davidson SD, Cavanagh AS, Bertrand JA, George SM. Molecular layer deposition of alucone polymer films using trimethylaluminum and ethylene glycol. *Chem Mater*. 2008;20:3315–3326.
21. Kubono A, Yuasa N, Shao HL, Umemoto S, Okui N. In-situ study on alternating vapor deposition polymerization of alkyl polyamide with normal molecular orientation. *Thin Solid Films*. 1996;289:107–111.
22. Shao HI, Umemoto S, Kikutani T, Okui N. Layer-by-layer polycondensation of nylon 66 by alternating vapour deposition polymerization. *Polymer*. 1997;38:459–462.
23. Kim A, Filler MA, Kim S, Bent SF. Layer-by-layer growth on Ge(100) via spontaneous urea coupling reactions. *J Am Chem Soc*. 2005;127:6123–6132.
24. Miyamae T, Tsukagoshi K, Matsuoka O, Yamamoto S, Nozoye H. Preparation of polyimide-polyamide random copolymer thin film by sequential vapor deposition polymerization. *Jap J Appl Phys Part 1*. 2002;41:746–748.
25. Yoshimura T, Ito S, Nakayama T, Matsumoto K. Orientation-controlled molecule-by-molecule polymer wire growth by the carrier-gas-type organic chemical vapor deposition and the molecular layer deposition. *Appl Phys Lett*. 2007;91:art No. 033103.
26. Putkonen M, Harjuoja J, Sajavaara T, Niinisto L. Atomic layer deposition of polyimide thin films. *J Mater Chem*. 2007;17:664–669.
27. Du Y, George SM. Molecular layer deposition of nylon 66 films examined using *in situ* FTIR spectroscopy. *J Phys Chem C*.2007;111:8509–8517.
28. Adarnczyk NM, Dameron AA, George SM. Molecular layer deposition of poly(p-phenylene terephthalamide) films using terephthaloyl chloride and p-phenylenediamine. *Langmuir*. 2008;24:2081–2089.
29. Wank JR, George SM, Weimer AW. Vibro-fluidization of fine boron nitride powder at low pressure. *Powder Technol*. 2001;121:195–204.
30. Hakim LF, Portman JL, Casper MD, Weimer AW. Aggregation behavior of nanoparticles in fluidized beds. *Powder Technol*. 2005;160:149–160.
31. Wank JR, George SM, Weimer AW. Coating fine nickel particles with Al_2O_3 utilizing an atomic layer deposition-fluidized bed reactor (ALD-FBR). *J Am Ceram Soc*. 2004;87:762–765.
32. Hakim LF, George SM, Weimer AW. Conformal nanocoating of zirconia nanoparticles by atomic layer deposition in a fluidized bed reactor. *Nanotechnology*. 2005;16:S375–S381.
33. Liang XH, George SM, Weimer AW, Li NH, Blackson JH, Harris JD, Li P. Synthesis of a novel porous polymer/ceramic composite material by low-temperature atomic layer deposition. *Chem Mater*. 2007;19:5388–5394.
34. Liang XH, Hakim LF, Zhan GD, McCormick JA, George SM, Weimer AW, Spencer JA, Buechler KJ, Blackson J, Wood CJ, Dorgan JR. Novel processing to produce polymer/ceramic nanocomposites by atomic layer deposition. *J Am Ceramic Soc*. 2007;90:57–63.
35. Liang XH, King DM, Groner MD, Blackson JH, Harris JD, George SM, Weimer AW. Barrier properties of polymer/alumina nanocomposite membranes fabricated by atomic layer deposition. *J Membr Sci*. 2008;322:105–112
36. King DM, Liang XH, Zhou Y, Carney CS, Hakim LF, Li P, Weimer AW. Atomic layer deposition of TiO_2 films on particles in a fluidized bed reactor. *Powder Technol*. 2008;183:356–363.
37. King DM, Spencer JA, Liang XH, Hakim LF, Weimer AW. Atomic layer deposition on particles using a fluidized bed reactor with in situ mass spectrometry. *Surf Coat Technol*. 2007;201:9163–9171.
38. McMahon CN, Alemany L, Callender RL, Bott SG, Barron AR. Reaction of Al(Bu-t)(3) with ethylene glycol: Intermediates to aluminum alkoxide (alucone) preceramic polymers. *Chem Mater*. 1999;11:3181–3188.
39. King DA, Wells MG. Reaction-mechanism in chemisorption kinetics-nitrogen on (100) plane of tungsten. Proceedings of the Royal Society of London Series A-Mathematical Physical and Engineering Sciences. 1974; 339:245–269.
40. Coon PA, Gupta P, Wise ML, George SM. Adsorption and desorption-kinetics for SiH_2Cl_2 on Si(111)7 $\times$ 7. *J Vac Sci Technol a-Vac Surf Films*. 1992;10:324–333.
41. Gupta P, Mak CH, Coon PA, George SM. Oxidation-kinetics of Si (111) 7x7 in the submonolayer regime. *Phys Rev B*. 1989;40:7739–7749.
42. Valverde JM, Castellanos A. Effect of vibration on agglomerate particulate fluidization. *AIChE J*. 2006;52:1705–1714.

Manuscript received Feb. 4, 2008, and revision received Oct. 1, 2008.